

Syntheses and Crystal Structures of *P*-Transition-Metalated Iminophosphoranes, $\text{Cp}^*(\text{CO})_2\text{M}\{\text{P}(\text{NPh})(\text{OMe})_2\}$ ($\text{M} = \text{Fe}$ and Ru)

Kazuyuki Kubo, Hiroshi Nakazawa,* Hiroyasu Inagaki, and Katsuhiko Miyoshi*

Department of Chemistry, Graduate School of Science, Hiroshima University,
Higashi-Hiroshima 739-8526, Japan

Received December 10, 2001

The reaction of $[\text{Cp}^*(\text{CO})_2\text{Fe}\{\text{P}(\text{NPh})(\text{OMe})_2\}]\text{PF}_6$ with NaNH_2 yielded the *P*-iron-bonded iminophosphorane $\text{Cp}^*(\text{CO})_2\text{Fe}\{\text{P}(\text{NPh})(\text{OMe})_2\}$, with deprotonation from the NPh group on the phosphorus. The ruthenium analogue, $\text{Cp}^*(\text{CO})_2\text{Ru}\{\text{P}(\text{NPh})(\text{OMe})_2\}$, was also prepared in a similar manner. The spectroscopic properties of the metallaiminophosphoranes are quite similar to those of their $\text{P}=\text{O}$ analogue, i.e., phosphonate complexes. The X-ray structure analyses revealed that the $\text{P}-\text{N}$ bond in $\text{Cp}^*(\text{CO})_2\text{Fe}\{\text{P}(\text{NPh})(\text{OMe})_2\}$ is comparable in length to that of the ruthenium analogue, $\text{Cp}^*(\text{CO})_2\text{Ru}\{\text{P}(\text{NPh})(\text{OMe})_2\}$, and both are considerably shorter than a $\text{P}-\text{N}$ single bond. These observations strongly suggest that the $\text{P}-\text{N}$ bonds in the *P*-metalated iminophosphoranes have substantial double-bond character. The structural features of the metallaiminophosphorane of iron resemble those of the starting cation complex, indicating that their electronic structures are basically similar. The iron-iminophosphorane is thermally stable compared with its Cp analogue, which is not stable enough to isolate, suggesting that both steric and electronic factors are responsible for the stability of the Cp^* complexes.

Introduction

Compounds bearing a phosphorus–nitrogen bond have attracted considerable attention in heteroatom chemistry.¹ In particular, iminophosphoranes ($\text{R}_3\text{P}=\text{NR}$), which make up an isoelectronic series with phosphorus ylides ($\text{R}_3\text{P}=\text{CR}_2$) and phosphine oxides ($\text{R}_3\text{P}=\text{O}$), have been extensively studied due to not only the basic interests in their structures and reactivity but also their availability as reagents for organic synthesis² and, more recently, as precursors to inorganic polymers.^{3,4} In addition, they have also been of great interest in coordination chemistry as ligands for transition metals. Iminophosphoranes bonded to a transition metal in η^1 fashion can be classified into three types: (i) *N*-coordinated iminophosphoranes with an *N*-metal dative bond,^{5–7} (ii) *N*-metalated iminophosphoranes with an *N*-metal covalent bond,^{6–8} and (iii) *P*-metalated iminophosphoranes with a *P*-metal covalent bond.

In contrast to many reports on the former two, those on the latter type are relatively rare.⁹ Although several *P*-metalated iminophosphoranes have been reported for

zirconium,¹⁰ iron,¹¹ cobalt,¹² palladium,¹³ and platinum,¹⁴ most of them were obtained unexpectedly in the

(5) For example, see: (a) Vicente, J.; Arcas, A.; Bautista, D.; Ramirez de Arellano, M. C. *Organometallics* **1998**, *17*, 4544, and references therein. (b) Ackermann, H.; Geiseler, G.; Harms, K.; Leo, R.; Massa, W.; Weller, F.; Dehnicke, K. *Z. Anorg. Allg. Chem.* **1999**, *625*, 1500. (c) Ackermann, H.; Leo, W.; Massa, W.; Dehnicke, K. *Z. Anorg. Allg. Chem.* **2000**, *626*, 608. (d) Krieger, M.; Gould, R. O.; Harms, K.; Greiner, A.; Dehnicke, K. *Z. Anorg. Allg. Chem.* **2001**, *627*, 747. (e) LePichon, L.; Stephan, D. W. *Inorg. Chem.* **2001**, *40*, 3827. (f) Stephens, J. C.; Khan, M. A.; Houser, R. P. *Inorg. Chem.* **2001**, *40*, 5064.

(6) For a review article, see: Dehnicke, K.; Krieger, M.; Massa, W. *Coord. Chem. Rev.* **1999**, *182*, 19.

(7) For example, see: (a) Schlecht, S.; Deubel, D. V.; Frenking, G.; Geiseler, G.; Harms, K.; Magull, J.; Dehnicke, K. *Z. Anorg. Allg. Chem.* **1999**, *625*, 887. (b) Gröb, T.; Seybert, G.; Massa, W.; Dehnicke, K. *Z. Anorg. Allg. Chem.* **2000**, *626*, 349.

(8) For recent examples, see: (a) Guérin, F.; Stephan, D. W. *Angew. Chem., Int. Ed.* **2000**, *39*, 1298. (b) Gröb, T.; Seybert, G.; Massa, W.; Weller, F.; Palaniswami, R.; Greiner, A.; Dehnicke, K. *Angew. Chem., Int. Ed.* **2000**, *39*, 4373. (c) Williams, V. C.; Müller, M.; Leech, M. A.; Denning, R. G.; Green, M. L. H. *Inorg. Chem.* **2000**, *39*, 2538. (d) Sung, R. C. W.; Courtenay, S.; McGarvey, B. R.; Stephan, D. W. *Inorg. Chem.* **2000**, *39*, 2542. (e) Carraz, C.-A.; Stephan, D. W. *Organometallics* **2000**, *19*, 3791. (f) Gröb, T.; Seybert, G.; Massa, W.; Harms, K.; Dehnicke, K. *Z. Anorg. Allg. Chem.* **2000**, *626*, 1361. (g) Dietrich, A.; Neumüller, B.; Dehnicke, K. *Z. Anorg. Allg. Chem.* **2000**, *626*, 1837. (h) Kickham, J. E.; Guérin, F.; Stewart, J. C.; Urbanska, E.; Stephan, D. W. *Organometallics* **2001**, *20*, 1175. (i) Courtenay, S.; Stephan, D. W. *Organometallics* **2001**, *20*, 1442. (j) Raab, M.; Sundermann, A.; Schick, G.; Loew, A.; Nieger, M.; Schoeller, W. W.; Niecke, E. *Organometallics* **2001**, *20*, 1770. (k) Yue, N. L. S.; Stephan, D. W. *Organometallics* **2001**, *20*, 2303. (l) Balakrishna, M. S.; Teipel, S.; Pinkerton, A. A.; Cavell, R. G. *Inorg. Chem.* **2001**, *40*, 1802. (m) Gröb, T.; Seybert, G.; Massa, W.; Dehnicke, K. *Z. Anorg. Allg. Chem.* **2001**, *627*, 304. (n) Balakrishna, M. S.; Teipel, S.; Pinkerton, A. A.; Cavell, R. G. *Inorg. Chem.* **2001**, *40*, 1802. (o) Guérin, F.; Beddie, C. L.; Stephan, D. W.; Spence, R. E. v. H.; Wurz, R. *Organometallics* **2001**, *20*, 3466. (p) Yue, N.; Hollink, E.; Guérin, F.; Stephan, D. W. *Organometallics* **2001**, *20*, 4424.

(9) A few *P*-metalated cyclic polyiminophosphoranes were reported by Allcock et al. For a review article, see: Allcock, H. R.; Desorcie, J. L.; Riding, G. H. *Polyhedron* **1987**, *6*, 119.

(10) For a review article, see: Majoral, J.-P.; Igau, A. *Coord. Chem. Rev.* **1998**, *176*, 1.

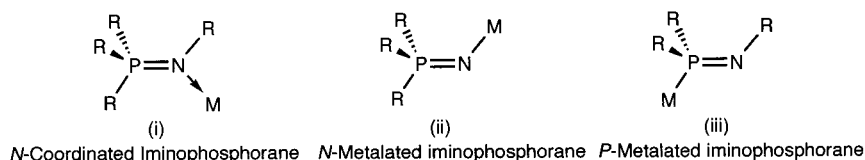
(1) (a) Emsley, J.; Hall, D. In *The Chemistry of Phosphorus*; Harper & Row: New York, 1976; Chapter 10. (b) Corbridge, D. E. C. In *Phosphorus. An Outline of its Chemistry, Biochemistry and Technology*; Elsevier: New York, 1980; Chapter 5.

(2) For review articles, see: (a) Gololobov, Y. G.; Kasukhin, L. F. *Tetrahedron* **1992**, *48*, 1353. (b) Molina, P.; Vilaplana, M. J. *Synthesis* **1994**, 1197.

(3) Wisian-Neilson, P., Allcock, H. R., Wynne, K. J., Eds. In *Inorganic and Organic Polymers II. Advanced Materials and Intermediates*; ACS Symposium Series 572; American Chemical Society: Washington, DC, 1994; Neilson, R. H., Jinkerson, D. L., Kucera, W. R., Longlet, J. J., Samuel, R. C., Wood, C. E., Chapter 18; White, M. L., Matyjaszewski, K., Chapter 24.

(4) For a review article, see: Manners, I. *Angew. Chem., Int. Ed. Engl.* **1996**, *35*, 1602.

Chart 1



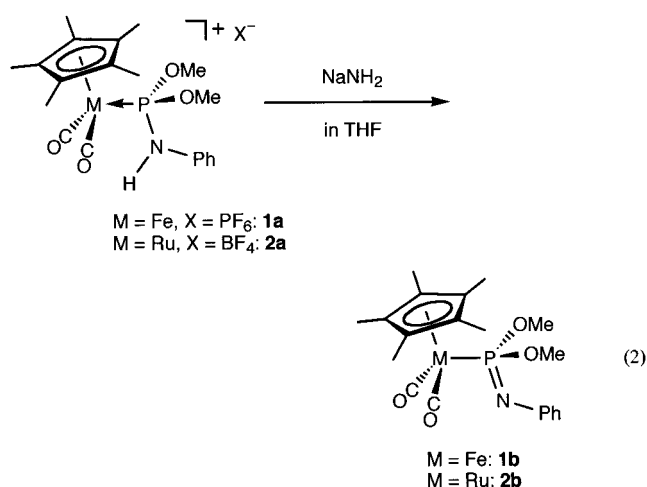
particular reactions. Therefore, the procedures adopted there have not been applied as a general synthetic method. In the case of the palladium complexes,¹³ the anionic compound $[\text{Ph}_2\text{PNP}(\text{O})\text{Ph}_2]^-$ was allowed to react with palladium complexes, yielding *P*-palladium-bonded iminophosphoranes. In this reaction, the anion serves as iminophosphoranide. This simple approach would be one of the good routes to the metalated iminophosphoranes. However, iminophosphoranide is usually in equilibrium with phosphinoamide, as shown in eq 1, and thus it also has the possibility of giving phosphinoamide complexes as well.



In this paper, we report the syntheses of *P*-metalated iminophosphoranes of iron and ruthenium by another simple and convenient procedure, which involves proton abstraction from cationic complexes having a $\text{P}\{\text{N}(\text{HPh})(\text{OMe})_2\}$ ligand. Although the similar deprotonation from phosphonium salts is known to be a facile route to organic iminophosphoranes, the reaction presented here is, to our knowledge, the first application to the preparation of transition-metalated iminophosphoranes. The spectroscopic and structural properties of the *P*-metalated iminophosphoranes are also reported.

Results and Discussion

Synthesis and Characterization of $\text{Cp}^*(\text{CO})_2\text{M}\{\text{P}(\text{NPh})(\text{OMe})_2\}$ ($\text{M} = \text{Fe}$ and Ru). The cationic iron-phosphite complex $[\text{Cp}^*(\text{CO})_2\text{Fe}\{\text{P}(\text{N}(\text{HPh})(\text{OMe})_2\})\text{PF}_6]$ (**1a**) (Cp^* stands for $\eta^5\text{-C}_5\text{Me}_5$), which was prepared in the reaction of $[\text{Cp}^*(\text{CO})_2\text{Fe}(\text{THF})]\text{PF}_6$ with $\text{P}\{\text{N}(\text{H}(\text{SiMe}_3))(\text{OMe})_2\}$ and then with H_2O , was dissolved in THF and then treated with an excess amount of NaNH_2 . During a few minutes stirring, the color of the solution changed from yellow to yellowish orange. The mixture was then worked up to give a yellow powder (eq 2). The ^{31}P NMR spectrum of the product showed a singlet at 122.3 ppm, which is at higher field than the chemical shift of the starting phosphite complex (161.5 ppm). No resonance due to the PF_6 counterion was observed. The two absorption bands (2016 and 1967 cm^{-1}) assignable to ν_{CO} in the IR spectrum appeared at lower frequency than those of the starting cation (2036 and 1991 cm^{-1}). In the ^1H NMR spectrum, the resonances attributed to $\text{C}_5(\text{CH}_3)_5$, OCH_3 , and NC_6H_5 protons were observed,



whereas an NH proton was not observed any longer. These observations strongly suggest that the N–H proton in **1a** was abstracted to form an electrically neutral complex with a $\text{P}(\text{V})$ fragment, that is, the *P*-iron-bonded iminophosphorane, $\text{Cp}^*(\text{CO})_2\text{Fe}\{\text{P}(\text{NPh})(\text{OMe})_2\}$ (**1b**) (68% yield). In addition, the X-ray crystallographic study (vide infra) confirmed the formation of **1b**.

The synthetic method presented here seems to be applicable to a wide range of transition-metal complexes. The cationic ruthenium-phosphite complex $[\text{Cp}^*(\text{CO})_2\text{Ru}\{\text{P}(\text{N}(\text{HPh})(\text{OMe})_2\})\text{BF}_4]$ (**2a**), which can be easily obtained from the reaction of $\text{Cp}^*(\text{CO})_2\text{RuCl}$ with $\text{P}\{\text{N}(\text{H}(\text{SiMe}_3))(\text{OMe})_2\}$, AgBF_4 , and then H_2O , is converted into the *P*-ruthenium-bonded iminophosphorane $\text{Cp}^*(\text{CO})_2\text{Ru}\{\text{P}(\text{NPh})(\text{OMe})_2\}$ (**2b**) (60% yield), in a manner similar to that of **1a**. Complex **2b** is the first example of a *P*-metalated iminophosphorane of ruthenium.

Although deprotonation from an aminophosphonium salt has been utilized in the preparation of a variety of organic iminophosphoranes,¹ there is no report so far on the deprotonation reaction of an aminophosphite coordinated to a cationic transition-metal complex. In this reaction, the phosphorus valence changes formally from $\text{P}(\text{III})$ to $\text{P}(\text{V})$, and the coordination mode of the phosphorus ligand concomitantly changes from dative to covalent. Since the starting complex has the phosphorus atom already bonded to the transition metal, the deprotonation from the nitrogen leads naturally to the exclusive formation of a *P*-metalated iminophosphorane.

Spectroscopic Properties of *P*-Metalated Iminophosphoranes. The ^{31}P NMR chemical shifts of $\text{Cp}^*(\text{CO})_2\text{M}\{\text{P}(\text{NPh})(\text{OMe})_2\}$ (122.3 ppm for $\text{M} = \text{Fe}$ (**1b**), 103.8 ppm for $\text{M} = \text{Ru}$ (**2b**)) are at lower field than those of the corresponding organic iminophosphoranes (-3 ppm for $\text{P}(\text{NPh})(\text{OMe})_3$ ¹⁵ and 16.7 ppm for $\text{PhP}(\text{NMe})_2$

(11) Newton, M. G.; King, R. B.; Chang, M.; Gimeno, J. *J. Am. Chem. Soc.* **1978**, *100*, 326.

(12) Pohl, D.; Ellermann, J.; Knoch, F. A.; Moll, M. *J. Organomet. Chem.* **1995**, *495*, C6.

(13) Smith, M. B.; Slawin, A. M. Z. *Polyhedron* **2000**, *19*, 695.

(14) Slawin, A. M. Z.; Smith, M. B.; Woollins, J. D. *J. Chem. Soc., Dalton Trans.* **1996**, 4567.

(15) Bellan, J.; Sanchez, M.; Marre-Mazieres, M. R.; Murillo, B. A. *Bull. Soc. Chim. Fr.* **1985**, 491.

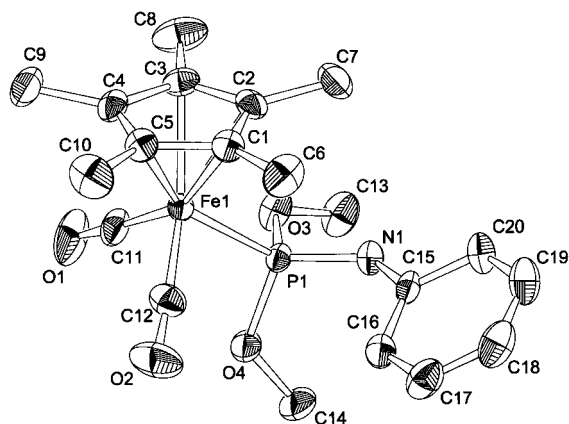


Figure 1. ORTEP drawing of **1b** showing the non-hydrogen atoms as 50% probability thermal ellipsoids with the numbering scheme. All hydrogen atoms are omitted for clarity.

(OMe)₂¹⁶), but they are close to that of the corresponding phosphonate complex Cp*(CO)₂FeP(O)(OMe)₂ (113.5 ppm).¹⁷ The IR data are also comparable to those of the phosphonate complex (ν_{CO} : 2016 and 1967 cm⁻¹ for **1b**, 2029 and 1976 cm⁻¹ for **2b**, 2014 and 1962 cm⁻¹ for Cp*(CO)₂FeP(O)(OMe)₂¹⁷). Therefore, it can be said that the iminophosphorane and phosphonate ligands provide similar electronic environments around the metal center. Comparison between ν_{CO} values of **1b** and **2b** in the IR spectra and of chemical shifts in the ³¹P NMR spectra reveals that the ruthenium complex has more electron-rich phosphorus and more electron-poor metal than does the iron complex. Indeed, the ¹H NMR spectrum of **2b** shows that the methyl protons in η^5 -C₅(CH₃)₅ are observed at slightly lower field, whereas the protons in the OMe groups on the phosphorus are observed at slightly higher field than those of **1b**. A similar tendency has been observed for the corresponding iron- and ruthenium-phosphonate complexes.¹⁸

X-ray Structures of 1a, 1b, and 2b. The X-ray crystal structures of *P*-metalated iminophosphoranes **1b** and **2b** were determined. The ORTEP drawings are given in Figures 1 and 2, respectively. For comparison, the X-ray structure of **1a** was also determined. In this case, the unit cell has two crystallographically independent molecules. The ORTEP drawing of one of the two is shown in Figure 3. The crystallographic data and selected bond distances and angles are summarized in Tables 1 and 2.

All complexes have typical piano-stool configurations with a Cp*, two carbonyls, and a phosphorus ligand all coordinated to the transition-metal center. The structural parameters of **1b** resemble closely those of **2b**, though each corresponding metal–ligand bond is longer for **2b**, probably due to the greater atomic radius of ruthenium. It should be emphasized that the P(1)–N(1) bond for **1b** (1.574(1) Å) is comparable in length to that for **2b** (1.575(2) Å), and both are considerably shorter

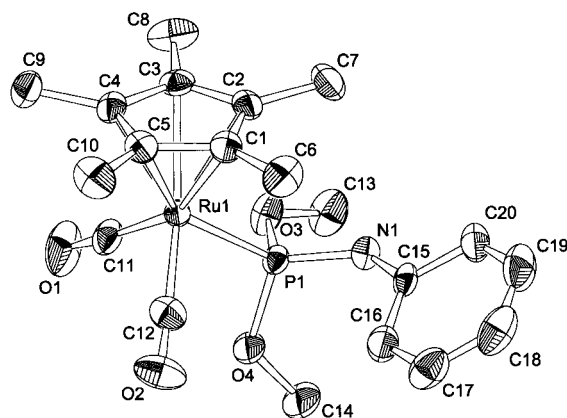


Figure 2. ORTEP drawing of **2b** showing the non-hydrogen atoms as 50% probability thermal ellipsoids with the numbering scheme. All hydrogen atoms are omitted for clarity.

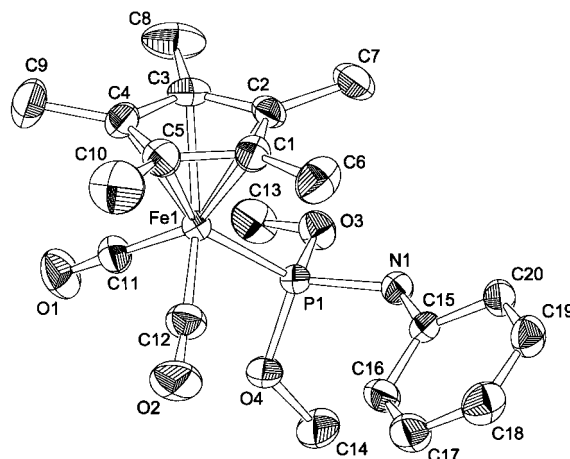


Figure 3. ORTEP drawing of one of the independent molecules of **1a** showing the non-hydrogen atoms as 50% probability thermal ellipsoids with the numbering scheme. All hydrogen atoms and the PF₆ counterion are omitted for clarity.

than a usual P–N single bond (ca. 1.78 Å).^{1a} These observations strongly suggest that the P–N bonds in **1b** and **2b** have substantial double-bond character. Furthermore, it should be noted that the P–N bond in **1a** (1.672(2) or 1.658(2) Å) is also relatively short, suggesting that it has already partial double-bond character. These three complexes take the common conformations around the M–P, P–N, and N–C bonds with the N atom sp²-hybridized (P(1)–N(1)–C(15) angles: **1b**, 130.2(1)°; **2b**, 128.8(2)°; **1a**, 125.1(2)° or 127.4(2)°). In all complexes, the Cp* and the two carbonyls on the transition-metal fragment are located in a staggered position around the M–P bond to the three substituents on the phosphorus fragment. The imino group is gauche to the Cp* ring and thus is trans to one of the two carbonyls (N(1)–P(1)–Fe(1)–C(11) torsion angle: **1b**, 174.1(1)°; **2b**, 172.4(1)°; **1a**, –172.7(1)° or –172.2(1)°). Similar conformational features were observed in the iron-phosphonate complexes Cp(CO)₂Fe{P(O)(OEt)₂}¹⁹ and Cp(CO)₂Fe{P(O)(CF₃)₂}²⁰ (Cp

(16) Goldwhite, H.; Gysegem, P.; Schow, S.; Swyke, C. *J. Chem. Soc., Dalton Trans.* **1975**, 12.

(17) Spectroscopic data for Cp*(CO)₂Fe{P(O)(OMe)₂}: IR (ν_{CO} , KBr disk): 2014, 1962 cm⁻¹. ¹H NMR (δ , in CDCl₃): 1.88 (s, 15H, C₅(CH₃)₅), 3.57 (d, J_{PH} = 12.0 Hz, 6H, OCH₃). ³¹P NMR (δ , in THF): 113.5 (s). Nakazawa, H.; Ichimura, S.; Nishihara, Y.; Miyoshi, K.; Nakashima, S.; Sakai, H. *Organometallics* **1998**, *17*, 5061.

(18) Nakazawa, H.; Fujita, T.; Kubo, K.; Miyoshi, K. *J. Organomet. Chem.* **1994**, *473*, 243.

(19) Nakazawa, H.; Morimasa, K.; Kushi, Y.; Yoneda, H. *Organometallics* **1988**, *7*, 458.

(20) (a) Barrow, M.; Sim, G. A. *J. Organomet. Chem.* **1974**, *69*, C4. (b) Barrow, M.; Sim, G. A. *J. Chem. Soc., Dalton Trans.* **1975**, 291.

Table 1. Summary of Crystal Data for **1a**, **1b**, and **2b**

	1a	1b	2b
formula	C ₂₀ H ₂₇ O ₄ NP ₂ F ₆ Fe	C ₂₀ H ₂₆ O ₄ NPF ₆ Fe	C ₂₀ H ₂₆ O ₄ NPRu
fw	577.22	431.25	476.47
color, habit	yellow, plate	yellow, stick	yellow, plate
cryst dimens, mm	0.30 × 0.30 × 0.25	0.28 × 0.25 × 0.30	0.38 × 0.15 × 0.08
cryst syst	orthorhombic	triclinic	triclinic
unit cell dimens			
<i>a</i> , Å	23.3290(4)	8.4470(3)	8.5940(2)
<i>b</i> , Å	8.7940(1)	10.2390(4)	10.3780(3)
<i>c</i> , Å	24.3940(2)	12.8300(5)	12.7040(4)
α, deg		84.362(2)	84.358(1)
β, deg		73.617(2)	74.460(2)
γ, deg		78.521(2)	77.377(2)
<i>V</i> , Å ³	5004.56(9)	1042.26(7)	1064.29(5)
space group	<i>Pca</i> 2 ₁ (#29)	<i>P</i> 1 (#2)	<i>P</i> 1 (#2)
<i>Z</i>	8	2	2
<i>D</i> _{calcd} , g m ⁻³	1.532	1.374	1.487
<i>F</i> (000)	2368.00	452.00	488.00
μ, cm ⁻¹	8.01	8.24	2.36
2θ _{max} , deg	55.9	55.8	55.5
no. of reflns			
measd	12 146	4615	4648
obsd (<i>I</i> > 3σ(<i>I</i>))	10742	4236	4362
struct soln	direct methods (SIR92)	direct methods (SAPI91)	Patterson methods (DIRDIF92 PATTY)
no. of params	615	349	349
<i>R</i> ^a	0.041	0.034	0.034
<i>R</i> _w ^b	0.065	0.057	0.052

^a $R = \sum ||F_o| - |F_c|| / \sum |F_o|$. ^b $R_w = [\sum w||F_o| - |F_c||^2 / \sum w|F_o|^2]^{1/2}$ and $w = 1/\sigma^2(F_o) = [o^2(F_o) + (p^2/4)F_o^2]^{-1}$.

Table 2. Selected Bond Lengths (Å) and Angles (deg) with Esd's in Parentheses for **1a**, **1b**, and **2b**

1a				1b		2b	
Fe(1)–P(1)	2.1864(6)	Fe(1')–P(1')	2.1854(6)	Fe(1)–P(1)	2.2218(4)	Ru(1)–P(1)	2.3189(5)
Fe(1)–C(11)	1.784(2)	Fe(1')–C(11')	1.775(3)	Fe(1)–C(11)	1.765(2)	Ru(1)–C(11)	1.883(3)
Fe(1)–C(12)	1.780(3)	Fe(1')–C(12')	1.776(3)	Fe(1)–C(12)	1.758(2)	Ru(1)–C(12)	1.889(3)
P(1)–O(3)	1.590(2)	P(1')–O(3')	1.580(2)	P(1)–O(3)	1.618(1)	P(1)–O(3)	1.615(2)
P(1)–O(4)	1.592(2)	P(1')–O(4')	1.590(2)	P(1)–O(4)	1.628(1)	P(1)–O(4)	1.625(2)
P(1)–N(1)	1.672(2)	P(1')–N(1')	1.658(2)	P(1)–N(1)	1.574(1)	P(1)–N(1)	1.575(2)
N(1)–C(15)	1.410(3)	N(1')–C(15')	1.414(3)	N(1)–C(15)	1.376(2)	N(1)–C(15)	1.381(3)
P(1)–Fe(1)–C(11)	91.37(8)	P(1')–Fe(1')–C(11')	90.57(8)	P(1)–Fe(1)–C(11)	87.45(6)	P(1)–Ru(1)–C(11)	86.48(8)
P(1)–Fe(1)–C(12)	93.21(9)	P(1')–Fe(1')–C(12')	93.65(9)	P(1)–Fe(1)–C(12)	90.12(7)	P(1)–Ru(1)–C(12)	88.79(8)
C(11)–Fe(1)–C(12)	93.9(1)	C(11')–Fe(1')–C(12')	94.7(1)	C(11)–Fe(1)–C(12)	95.25(9)	C(11)–Ru(1)–C(12)	92.3(1)
Fe(1)–P(1)–O(3)	118.20(7)	Fe(1')–P(1')–O(3')	117.92(8)	Fe(1)–P(1)–O(3)	105.98(5)	Ru(1)–P(1)–O(3)	106.03(7)
Fe(1)–P(1)–O(4)	106.63(7)	Fe(1')–P(1')–O(4')	107.29(8)	Fe(1)–P(1)–O(4)	103.65(5)	Ru(1)–P(1)–O(4)	104.79(7)
Fe(1)–P(1)–N(1)	122.21(8)	Fe(1')–P(1')–N(1')	121.89(8)	Fe(1)–P(1)–N(1)	125.10(6)	Ru(1)–P(1)–N(1)	123.54(8)
O(3)–P(1)–O(4)	107.02(9)	O(3')–P(1')–O(4')	106.9(1)	O(3)–P(1)–O(4)	103.06(8)	O(3)–P(1)–O(4)	103.5(1)
O(3)–P(1)–N(1)	94.6(1)	O(3')–P(1')–N(1')	94.0(1)	O(3)–P(1)–N(1)	104.27(7)	O(3)–P(1)–N(1)	104.0(1)
O(4)–P(1)–N(1)	106.90(9)	O(4')–P(1')–N(1')	107.5(1)	O(4)–P(1)–N(1)	112.62(8)	O(4)–P(1)–N(1)	113.1(1)
P(1)–N(1)–C(15)	125.1(2)	P(1')–N(1')–C(15')	127.4(2)	P(1)–N(1)–C(15)	130.2(1)	P(1)–N(1)–C(15)	128.8(2)

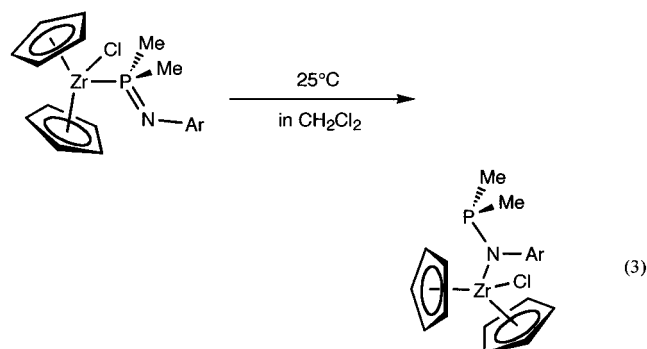
stands for η^5 -C₅H₅), in which the phosphoryl oxygen is trans to one of the two carbonyls, suggesting that this conformation is general for the complexes of the type $[(\eta^5\text{-C}_5\text{R}_5)(\text{CO})_2\text{M}\{\text{P}(\text{E})\text{R}'_2\}]^{n+}$ (M = Fe, Ru; E = O, NR, NHR; *n* = 0, 1), irrespective of steric demands of substituents on the phosphorus and of the charge on the molecule. Therefore, it seems that some preferable orbital interactions are responsible for the common conformation, and this implies that **1a** and **1b** (and also **2b**) have closely related electronic structures. In other words, even though the deprotonation from the amino group in **1a** leads to formal changes in phosphorus valency from P(III) to P(V) and in a metal–phosphorus bonding from dative to covalent, the basic molecular orbital compositions would not be significantly changed.

The Fe(1)–P(1) bond is slightly longer in **1b** (2.2218(4) Å) than in **1a** (2.1864(6) or 2.1854(6) Å). Thus, it can be proposed that the deprotonation from **1a** to give **1b** causes slight weakening of the metal–phosphorus bond, although the anionic iminophosphorane ligand in **1b**

may be greater in σ -donacity than the electrically neutral phosphite ligand in **1a**. This observation can be rationally explained as follows. As mentioned above, **1a** and **1b** might have similar electronic structure with somewhat larger P–N double-bond character in **1b**, and the π bond is made up of the filled π orbital on the N atom and the empty σ^* orbital on the P atom. Therefore, the stronger π bonding in **1b** would lead to greater electron distribution into the σ^* orbital, leading to the weaker phosphorus–substituent (other than the imino group) bonds in **1b**. Indeed, the P–OMe bonds are also slightly longer in **1b** than in **1a**.

Stability and Reactivity of P-Metalated Imino-phosphoranes. The metalated iminophosphoranes **1b** and **2b** are both air- and/or moisture-sensitive but neither decomposition nor rearrangement is observed under an inert atmosphere and at least up to 60 °C in benzene. In contrast, a *P*-zirconium-bonded iminophosphorane has been reported to be converted into a phosphinoamide complex at 25 °C via migration of the

zirconium fragment from P to N (eq 3).²¹ The difference

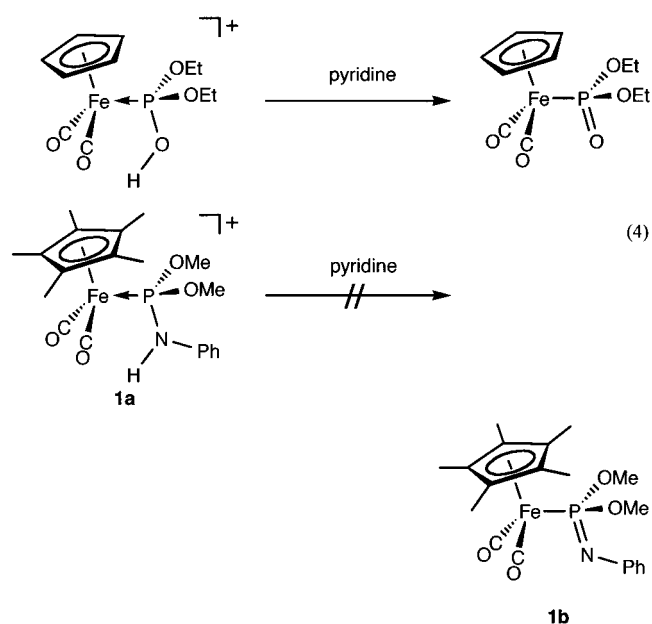


in the thermal stability can be rationalized from the HSAB concept. That is, the anionic ligand $[R_2PNR]^-$ can be described as a resonance hybrid of iminophosphorane and phosphinoamide (eq 1), though a theoretical study revealed that the latter prevails in equilibrium in usual cases.²² Since the zirconium fragment $[(Cp)_2ZrCl]^+$ would serve as a hard acid, it prefers hard *N*-coordination to soft *P*-coordination, resulting eventually in exclusive formation of a phosphinoamide complex. In contrast, the iron and ruthenium fragments $[(Cp^*(CO)_2M]^+$ may serve as a soft acid, and so they would preferably coordinate to the phosphorus atom to give *P*-metalated iminophosphoranes. Thus, it could be proposed that fragments of the late transition metals in a low oxidation state are stabilized by *P*-coordination of the iminophosphorane, while those of early transition metals in a high oxidation state by *N*-coordination of phosphinoamides. Indeed, the anionic compound $[Ph_2PNP(O)Ph_2]^-$ reacted with palladium complexes, i.e., soft acids, to yield not *N*- (nor *O*-) coordinated complexes but *P*-palladium-bonded iminophosphoranes.¹⁴

To examine the stability of the metalated iminophosphorane having a Cp ligand in place of a Cp^* ligand, the preparation of the Cp analogue of **1b**, $Cp(CO)_2Fe\{P(NPh)(OMe)_2\}$, was attempted. Since the reaction of $NaNH_2$ with the cationic complex $[Cp(CO)_2Fe\{P(NHPh)(OMe)_2\}]PF_6$ gave many unknown products, $LiN(SiMe_3)_2$ was then used as a milder base. The reaction mixture at $-78^\circ C$ showed a resonance at 99.8 ppm in the ^{31}P NMR spectrum as a sole product. This chemical shift was indicative of the formation of the metalated iminophosphorane $Cp(CO)_2Fe\{P(NPh)(OMe)_2\}$. However, the product is not stable enough to isolate, and decomposition took place at room temperature. Therefore, it can be considered that the Cp^* ligand plays an important role in the stabilization of the present metalated iminophosphoranes. In addition to the kinetic stabilization due to the bulkiness of the Cp^* ligand, an electronic factor also seems to be responsible. Since the Cp^* ligand is a stronger electron donor than Cp , it makes the transition-metal center more electron-rich. Therefore, the back-donation from the metal center to the iminophosphorane ligand is greater for the Cp^* complex, leading to a stronger metal–phosphorus bond. The presence of this greater back-donation in the Cp^*

complex was supported by ^{31}P NMR considerations. Our previous study on the metallaphosphorane $Cp(CO)LFe\{P(OC_6H_4NH_2)_2\}$, containing highly polarized $P-O_{apical}$ bonds, revealed that the π back-donation from the transition-metal fragment increases the polarization of the phosphorus–substituent bond to accumulate a positive charge on the phosphorus, leading to the downfield shift in the ^{31}P NMR.²³ Similar explanations could be applied to the present case. That is, the Cp^* complex **1b** resonates at lower field (122.3 ppm) than its Cp analogue (99.8 ppm), because the greater π back-donation in **1b** polarizes the $P=N$ bond more, leading to more positive charge on the phosphorus.

It was previously reported that a protonated iron-phosphonate complex, i.e., a cationic phosphite complex, can be deprotonated by relatively mild bases such as pyridine.¹⁹ In contrast, the protonated **1b**, i.e., **1a**, is not deprotonated by pyridine (eq 4) under similar conditions. This suggests that the nitrogen atom in **1b** is more



basic than the phosphoryl oxygen in the phosphonate complex. A similar trend is generally observed between organic iminophosphoranes and phosphonates.^{1b} Therefore, it can be expected that the *P*-metalated iminophosphoranes are more reactive toward electrophiles than the corresponding phosphonate complexes.²⁴ This means that the *P*-metalated iminophosphoranes could serve as good ligands to provide novel binuclear transition-metal complexes with *N*-coordination as in type (i) and (ii) in Chart 1.

Experimental Section

All reactions were carried out under an atmosphere of dry nitrogen using standard Schlenk techniques. Column chromatography was done quickly in the air. THF, diethyl ether, and benzene were distilled from sodium metal, whereas CH_2Cl_2 was distilled from P_2O_5 , and then they were stored under a dry nitrogen atmosphere. Other organic solvents, $AgBF_4$ and

(21) (a) Igau, A.; Dufour, N.; Mahieu, A.; Majoral, J.-P. *Angew. Chem., Int. Ed. Engl.* **1993**, *32*, 95. (b) Mahieu, A.; Igau, A.; Jaud, J.; Majoral, J.-P. *Organometallics* **1995**, *14*, 944.

(22) Trinquier, G.; Ashby, M. T. *Inorg. Chem.* **1994**, *33*, 1306.

(23) Kubo, K.; Nakazawa, H.; Mizuta, T.; Miyoshi, K. *Organometallics* **1998**, *17*, 3522.

(24) (a) Nakazawa, H.; Kadoi, Y.; Itoh, T.; Mizuta, T.; Miyoshi, K. *Organometallics* **1991**, *10*, 766. (b) Kubo, K.; Nakazawa, H.; Nakahara, S.; Yoshino, K.; Mizuta, T.; Miyoshi, K. *Organometallics* **2000**, *19*, 4932.

NaNH₂, were obtained from common commercial sources and used without further purification. HNPh(SiMe₃)₂,²⁵ [Cp*(CO)₂-Fe(THF)]PF₆,²⁶ and Cp*(CO)₂RuCl²⁷ were prepared in accordance with published procedures.

HPLC was performed using a JAI LC-908 recycling preparative HPLC instrument with JAIGEL-1H and -2H columns and with CHCl₃ as eluent. IR spectra were recorded on either a Shimadzu FTIR-8100A or a Perkin-Elmer Spectrum One spectrometer. A JEOL LA-300 multinuclear spectrometer was used to obtain ¹H, ¹³C, and ³¹P NMR spectra. ¹H and ¹³C NMR data were referenced to Me₄Si, and ³¹P NMR data were referenced to 85% H₃PO₄. Elemental analysis data were obtained on a Perkin-Elmer 2400 CHN elemental analyzer.

Preparation of P{NPh(SiMe₃)}(OMe)₂. The ether solution (80 mL) of LiNPh(SiMe₃) was prepared from the reaction of HNPh(SiMe₃) (10.22 g, 61.8 mmol) with n-BuLi (2.47 M hexane solution, 25.0 mL, 61.8 mmol) at -78 °C. To the solution was added the ether solution (100 mL) of P(OMe)₂Cl (5.6 mL, 62.6 mmol) at -78 °C, which was prepared by overnight stirring of PCl₃ (1.8 mL, 20.6 mmol) with P(OMe)₃ (4.0 mL, 33.9 mmol) at room temperature. After stirring for 2 h at room temperature, the volatile components were removed under vacuum. Finally, distillation at 80 °C under reduced pressure (60 Pa) provided P{NPh(SiMe₃)}(OMe)₂ (6.85 g, 26.6 mmol, 43% yield) with a small amount of impurities. It can be used in the following reactions without further purification. ¹H NMR (δ, in CDCl₃): 0.29 (d, J_{PH} = 1.5 Hz, 9H, SiCH₃), 3.55 (d, J_{PH} = 12.6 Hz, 6H, OCH₃), 7.08–7.37 (m, 5H, C₆H₅). ¹³C NMR (δ, in CDCl₃): 1.19 (d, J_{PC} = 7.5 Hz, SiCH₃), 50.41 (d, J_{PC} = 18.0 Hz, OCH₃), 124.93 (s, C₆H₅), 128.18 (s, C₆H₅), 130.12 (d, J_{PC} = 3.1 Hz, C₆H₅), 140.65 (d, J_{PC} = 3.7 Hz, C₆H₅). ³¹P NMR (δ, in CDCl₃): 145.35 (s).

Preparation of [Cp*(CO)₂Fe{P(NHPh)(OMe)₂}]PF₆ (1a). [Cp*(CO)₂Fe(THF)]PF₆ (3.68 g, 7.92 mmol) was dissolved in CH₂Cl₂ (75 mL) and treated with P(OMe)₂{NPh(SiMe₃)} (2.10 mL, 7.92 mmol) at room temperature. The mixture was stirred overnight, and then a few drops of H₂O were added. After stirring for an additional 2 h, the mixture was loaded on a silica gel column and eluted with CH₂Cl₂ and then with CH₂Cl₂/acetone, 1:4. A pale yellow band eluted with 1:4 CH₂Cl₂/acetone was collected and dried under vacuum to give a yellow oil. The oil was dissolved in a small amount of THF, and then a large amount of ether was added to form a pale yellow precipitate. After washing with ether several times, the precipitate was dried under reduced pressure to give [Cp*(CO)₂-Fe{P(NHPh)(OMe)₂}]PF₆, **1a**, as a yellow powder (3.07 g, 5.32 mmol, 67% yield). Anal. Calcd for C₂₀H₂₇O₄NPF₆Fe: C, 41.62; H, 4.71; N, 2.43. Found: C, 41.67; H, 4.70; N, 2.36. IR (ν_{CO}, in THF): 2036, 1991 cm⁻¹. ¹H NMR (δ, in CDCl₃): 1.74 (s, 15H, C₅(CH₃)₅), 3.82 (d, J_{PH} = 12.1 Hz, 6H, OCH₃), 6.22 (br d, J_{PH} = 3.9 Hz, 1H, NH), 7.08–7.30 (m, 5H, C₆H₅). ¹³C NMR (δ, in CDCl₃): 9.17 (s, C₅(CH₃)₅), 54.12 (d, J_{CP} = 8.7 Hz, OCH₃), 100.42 (s, C₅(CH₃)₅), 119.27 (d, J_{CP} = 6.2 Hz, C₆H₅), 123.46 (s, C₆H₅), 129.81 (s, C₆H₅), 138.03 (d, J_{CP} = 4.9 Hz, C₆H₅), 211.05 (d, J_{CP} = 34.10 Hz, CO). ³¹P NMR (δ, in CDCl₃): 161.5 (s, Fe-P), -143.9 (sep, J_{PF} = 712.0 Hz, PF₆⁻).

Preparation of [Cp*(CO)₂Ru{P(NHPh)(OMe)₂}]BF₄ (2a). To the mixture of Cp*(CO)₂RuCl (232 mg, 0.71 mmol) and AgBF₄ (138 mg, 0.71 mmol) in 15 mL of CH₂Cl₂ was added dropwise 10 mL of a CH₂Cl₂ solution of P(OMe)₂{NPh(SiMe₃)} (1.19 mL, 0.71 mmol) at room temperature. After stirring for 1.5 h, the mixture was filtered and the volatile components were removed from the filtrate under reduced pressure. The residue was washed with ether several times and dissolved in 15 mL of CH₂Cl₂, and then a few drops of H₂O were added. The mixture was stirred for 1.5 days, and then the volatile

components were removed under vacuum. The residue was dissolved in a small amount of CH₂Cl₂ and loaded on a silica gel column, and then all the eluents with a mixture of CH₂Cl₂/acetone (4/1) were collected and dried. The pure Cp*(CO)₂Ru{P(NHPh)(OMe)₂} (**2a**) was finally obtained by GLPC separation as a white powder (182 mg, 0.32 mmol, 46% yield). Anal. Calcd for C₂₀H₂₇O₄NBF₄Pr: C, 42.57; H, 4.82; N, 2.48. Found: C, 42.69; H, 4.90; N, 2.41. IR (ν_{CO}, in THF): 2050, 1002 cm⁻¹. ¹H NMR (δ, in CDCl₃): 1.85 (s, 15H, C₅(CH₃)₅), 3.72 (d, J_{PH} = 12.3 Hz, 6H, OCH₃), 6.97–7.29 (m, 5H, C₆H₅). The signal due to the NH proton was not observed, probably because of broadening and/or overlapping with the multiplet due to phenyl protons. ¹³C NMR (δ, in CDCl₃): 10.09 (s, C₅(CH₃)₅), 53.91 (d, J_{CP} = 7.5 Hz, OCH₃), 103.35 (s, C₅(CH₃)₅), 119.28 (d, J_{CP} = 6.8 Hz, C₆H₅), 122.96 (s, C₆H₅), 129.54 (s, C₆H₅), 138.64 (d, J_{CP} = 3.7 Hz, C₆H₅), 197.51 (d, J_{CP} = 30.4 Hz, CO). ³¹P NMR (δ, in CDCl₃): 136.7 (s).

Preparation of Cp*(CO)₂Fe{P(NHPh)(OMe)₂} (1b). To a yellow solution of **1a** (419 mg, 0.73 mmol) in THF (30 mL) was added an excess amount of NaNH₂, and the mixture was stirred at room temperature for 30 min. The color of the solution changed to yellowish orange. After volatile components were removed under reduced pressure, the product was extracted with pentane from the residue. Finally the solvent was removed in vacuo to give Cp*(CO)₂Fe{P(NHPh)(OMe)₂} (**1b**) as an orange-yellow powder (213 mg, 0.49 mmol, 68% yield). When the product has reddish color, it should be washed with a small amount of hexane. Anal. Calcd for C₂₀H₂₆O₄NPF₆Fe: C, 55.70; H, 6.08; N, 3.25. Found: C, 55.81; H, 5.63; N, 3.11. IR (ν_{CO}, in THF): 2016, 1967 cm⁻¹. ¹H NMR (δ, in CDCl₃): 1.71 (s, 15H, C₅(CH₃)₅), 3.65 (d, J_{PH} = 11.4 Hz, 6H, OCH₃), 6.61–7.12 (m, 5H, C₆H₅). ¹³C NMR (δ, in CDCl₃): 9.44 (s, C₅(CH₃)₅), 51.61 (d, J_{CP} = 8.7 Hz, OCH₃), 98.16 (s, C₅(CH₃)₅), 116.58 (s, C₆H₅), 122.96 (d, J_{CP} = 17.4 Hz, C₆H₅), 128.63 (s, C₆H₅), 150.60 (d, J_{CP} = 6.26 Hz, C₆H₅), 214.47 (d, J_{CP} = 35.18 Hz, CO). ³¹P NMR (δ, in CDCl₃): 122.3 (s).

Preparation of Cp*(CO)₂Ru{P(NHPh)(OMe)₂} (2b). Using **2a** (182 mg, 0.32 mmol) as a starting material, Cp*(CO)₂Ru{P(NHPh)(OMe)₂} (**2b**) was prepared as a yellow powder by a procedure similar to that for **1b** (92 mg, 0.19 mmol, 60% yield). Anal. Calcd for C₂₀H₂₆O₄NPr: C, 50.42; H, 5.50; N, 2.94. Found: C, 49.83; H, 5.74; N, 2.66. IR (ν_{CO}, in THF): 2029, 1976 cm⁻¹. ¹H NMR (δ, in CDCl₃): 1.83 (s, 15H, C₅(CH₃)₅), 3.57 (d, J_{PH} = 12.1 Hz, 6H, OCH₃), 6.64–7.11 (m, 5H, C₆H₅). ¹³C NMR (δ, in CDCl₃): 9.88 (s, C₅(CH₃)₅), 50.59 (d, J_{CP} = 6.2 Hz, OCH₃), 101.86 (s, C₅(CH₃)₅), 116.37 (s, C₆H₅), 122.99 (d, J_{CP} = 18.0 Hz, C₆H₅), 128.57 (s, C₆H₅), 150.83 (d, J_{CP} = 9.9 Hz, C₆H₅), 200.59 (d, J_{CP} = 18.6 Hz, CO). ³¹P NMR (δ, in CDCl₃): 103.8 (s).

X-ray Structure Determination for 1a, 1b, and 2b. A suitable crystal of **1a** was obtained through recrystallization from CH₂Cl₂, while those of **1b** and **2b** were obtained from benzene, and then they were separately mounted on a glass fiber. All measurements were made on a Mac Science DIP2030 diffractometer with graphite-monochromated Mo Kα radiation (λ = 0.710 73 Å) at 200 K. Crystal data, data collection parameters, and results of the analyses are summarized in Table 1.

The structures were solved by direct methods with the program SIR92²⁸ for **1a** and SAPI91²⁹ for **1b** and by the Patterson method for **2b** with the program DIRDIF92 PATTY³⁰ and then were expanded using Fourier techniques.³¹ Positions

(28) Altomare, A.; Burla, M. C.; Camalli, M.; Cascarano, M.; Giacovazzo, C.; Guagliardi, A.; Polidori, G. *J. Appl. Crystallogr.* **1994**, *27*, 435.

(29) Fan, H.-F. *Structure Analysis Programs with Intelligent Control*; Rigaku Corporation: Tokyo, Japan, 1991.

(30) Beurskens, P. T.; Admiral, G.; Beurskens, G.; Bosman, W. P.; Garcia-Granda, S.; Gould, R. O.; Smits, J. M. M.; Smykalla, C. *The DIRDIF program system*; Technical Report of the Crystallography Laboratory; University of Nijmegen: Nijmegen, The Netherlands, 1992.

(25) Randall, E. W.; Zuckerman, J. J. *J. Am. Chem. Soc.* **1968**, *90*, 3167.

(26) Catheline, D.; Astruc, D. *Organometallics* **1984**, *3*, 1094.

(27) Blockmore, T.; Cotton, J. G.; Bruce, M. I.; Stone, F. G. A. *J. Chem. Soc. A* **1968**, 2931.

of hydrogen atoms of **1a** were calculated by assuming idealized geometries, whereas those of **1b** and **2b** were determined from subsequent difference Fourier maps. The non-hydrogen atoms were refined anisotropically. Hydrogen atoms were not refined for **1a**, but they were refined isotropically for **1b** and **2b**. An extinction correction was applied in each case. Neutral atom scattering factors were taken from Cromer and Waber.³² Anomalous dispersion effects were included in F_{calc} ,³³ the values for $\Delta f'$ and $\Delta f''$ were those of Creagh and McAuley.³⁴ The values for the mass attenuation coefficients are those of

(31) Beurskens, P. T.; Admiraal, G.; Beurskens, G.; Bosman, W. P.; de Gelder, R.; Israel, R.; Smits, J. M. M. *The DIRDIF-94 program system*; Technical Report of the Crystallography Laboratory; University of Nijmegen: Nijmegen, The Netherlands, 1994.

(32) Cromer, D. T.; Waber, J. T. In *International Tables for X-ray Crystallography*; The Kynoch Press: England, 1974; Vol. IV, Table 2.2A.

(33) Ibers, J. A.; Hamilton, W. C. *Acta Crystallogr.* **1964**, *17*, 781.

(34) Creagh, D. C.; McAuley, W. J. In *International Tables for Crystallography*; Wilson, A. J. C., Ed.; Kluwer Academic Publishers: Boston, 1992; Vol. C, Table 4.2.6.8.

Creagh and Hubbel.³⁵ All calculations were performed using the program package *teXsan*.³⁶

Acknowledgment. This work was supported by Grants-in-Aid for Scientific Research (Nos. 11740371 and 12640539) from the Ministry of Education, Culture, Sports, Science and Technology of Japan.

Supporting Information Available: Details of X-ray crystal structure determination of **1a**, **1b**, and **2b** including tables of intensity collection and refinement details, atomic coordinates and thermal parameters, and bond distances and angles. This material is available free of charge via the Internet at <http://pubs.acs.org>.

OM0110484

(35) Creagh, D. C.; Hubbel, J. H. In *International Tables for Crystallography*; Wilson, A. J. C., Ed.; Kluwer Academic Publishers: Boston, 1992; Vol. C, Table 4.2.4.3.

(36) *teXsan*, A Crystal Structure Analysis Package; Molecular Structure Corporation: The Woodlands, TX, 1985 and 1992.